Available online at website: https://journal.bcrec.id/index.php/bcrec

Bulletin of Chemical Reaction Engineering & Catalysis, 21 (1) 2026, 51-67

Original Research Article

Adsorptive Removal of Cd(II) Ions using Core-Shell Polystyrene@NiFeAl-LDH Nanocomposite: Optimization, Isotherm, and Kinetics Study

Shahad A. Raheem[1*], Ahmed A. Mohammed[2]

[1]Civil Engineering Department, College of Engineering, Al-Qasim Green University, Babylon 51013, Iraq.
[2]Department of Environmental Engineering, University of Baghdad, Iraq

Received: 5th November 2025; Revised: 26th November 2025; Accepted: 28th November 2025
Available online: 8th December 2025; Published regularly: April 2026

Abstract

In this study, a core-shell nanocomposite was successfully prepared using NiAlFe-LDH as a core coated with polystyrene (PS) nanoparticles with an LDH:PS ratio of 3:1 (PS @NiAlFe-LDH) for the removal of cadmium (Cd^{2+}) from aqueous solutions. PS nanospheres were prepared from styrene monomer recovered from Styrofoam waste. The prepared PS@NiAlFe-LDH was characterized for its structural morphology, elemental composition, surface area, and pore morphology. Results indicated the successful formation of PS nanosphers core coated by platelet LDH shell and a successful adsorption of Cd^{2+} ions. The maximum adsorption efficiency (95.53%) was achieved under the optimal conditions: pH of 6, PS@NiAlFe-LDH dosage of 0.15 g/100 mL, shaking speed of 200 rpm, and an initial Cd^{2+} concentration of 100 mg/L at a 90-minute contact time. Langmuir isotherm model was the most accurate in describing the adsorption process with a maximum adsorption capacity of 227.273 mg/g. The pseudo-second-order (PSO) kinetics model described the adsorption behaviour of cadmium ions on PS@NiAlFe-LDH surface as the calculated values from the model were close to the experimental values. The adsorption mechanism was a combination of electrostatic attraction, surface complexation/ion exchange and internal diffusion within the pores. PS@NiAlFe-LDH demonstrated significant reusability, with an efficiency of 57.56% after six regeneration cycles. In conclusion, this study indicates that PS@NiAlFe-LDH nanocomposite exhibits high quality and excellent efficiency in removing cadmium ions from aqueous solutions, owing to its porosity and abundance of active groups on its surface, as well as structural stability after adsorption, which makes it a promising material for environmental remediation applications.

Keywords: Polystyrene; Layered double hydroxide; Styrofoam; Nanocomposites; Adsorption

How to Cite: Raheem, S. A., Mohammed, A. A. (2026). Adsorptive Removal of Cd(II) Ions using Core-Shell Polystyrene@NiFeAl-LDH Nanocomposite: Optimization, Isotherm, and Kinetics Study. *Bulletin of Chemical Reaction Engineering & Catalysis*, 21(1), 51-67. (doi: 10.9767/bcrec.20528)

Permalink/DOI: https://doi.org/10.9767/bcrec.20528

1. Introduction

The rapid increase in industrial activity has prompted heavy metal contamination of the environment [1]. Cadmium (Cd) is one of the most toxic elements to humans and is commonly used in many industrial activities, including alloy manufacturing, smelting, electroplating, pigments, plastics, and battery manufacturing [2]. Ecosystems readily absorb cadmium and then accumulate it in people through the food chain, where it has been linked to cancer, hypertension, renal dysfunction, and liver disorders [3]. According to the World Health Organization (WHO), the maximum level of Cd^{2+} contamination in drinking water should not exceed 0.003 mg/L [4]. Many technologies can be used to remove Cd^{2+} from aqueous solutions, including adsorption [5], membrane filtration [6], ion exchange [7], and

* Corresponding Author.
Email: shahad.ak@wrec.uoqasim.edu.iq (S.A. Raheem)

chemical precipitation [8]. Among these methods, adsorption is an efficient and economical approach due to its simplicity, ease of operation, cost-effectiveness, and excellent removal efficiency [9]. The efficiency of adsorption depends on the properties of the adsorbent, such as surface area and the availability of binding sites [10]. Thus, many materials have been synthesized, modified, and tested as adsorbents for heavy metal ions [11]. The cost-effectiveness of adsorption depends on the nature of the adsorbent; therefore, researchers are continually searching for inexpensive and efficient materials [12]. Styrofoam or expanded polystyrene (EPS) is a thermoplastic material prepared from a petroleum-based product (styrene), developed into PS by polymerization. Styrofoam is used in food packaging, household appliances, and disposable products in material packaging, leading to a significant increase in styrofoam waste [13]. However, it has become a critical environmental issue due to its non-decomposable nature and persistent environmental presence, posing risks through accumulative visual pollution, ecological disturbances, and probable health dangers [14]. The methods used to remediate plastic waste contamination may include direct dumping or landfilling, incineration, and mechanical recycling. Landfilling of these waste into the soil has a long-term effects as degredation over time produces a microplastic fragments that have potential impact on the ecosystem [15]. Incineration of styrofoam waste leads to the emission of harmful gases, such as benzene, toluene, and xylene, that humans and animals can inhale, causing diverse kinds of cancer, lung disease, and immune disorders [16]. Mechanical recycling converts styrofoam waste into products with similar purposes. Consequently, there is an emergent necessity to realize the adverse effects of Styrofoam waste and develop sustainable methods for its management [17]. One way is to develop a valuable products from Styrofoam waste.

Soheilian *et al*. used PS nanoparticles for the adsorption of copper. With a maximum adsorption capacity of 6.36 mg/g [18]. Researchers found that PS nanoparticles could be used with another material to increase its adsorption capacity [19–21]. Hence, in this research, Styrofoam waste was converted into polystyrene nanosphers (PS) and embedded with layered double hydroxide (LDH) which have attracted attention as potentially efficient adsorbents in removing heavy metal ions due to their characteristics such as organized layered configuration, high surface area, excellent ion exchange properties, and easy to deal with in composition [22,23], to develop a core-shell nanocomposite in which PS nanosphers core is coated with NiAlFe-LDH shell (PS@NiAlFe-LDH). Along with the sustainable reuse of styrofoam waste, embedding PS nanosphers with LDH create a more stable material, can significantly increase the specific surface area, which enhances the adsorption capacity. The LDH shell prevents the adhesion and agglomeration of PS nanosphers, allowing the well-distribution of nanocomposite and facilitate the diffution of Cadmium, thus increasing the adsorption capacity. LDH contains -OH groups, M^{2+} and M^{3+} cations (such as: Mg^{2+}, Al^{3+}, Ni^{2+}, and Fe^{3+}), cadmium can bind strongly to these sites via complexation and electrostatic attraction which results in stronger and more stable adsorption compared to PS nanosphers alone.The physio-chemical characteristics of the prepared nanocomposite were examined using transmission electrons microscopy (TEM), X-ray diffraction patterns (XRD), scanning-electron-microscopy/energy-dispersive X-ray spectroscopy (SED/EDX), Brunauer-Emmett-Teller analysis (BET), and Fourier-transform-infrared-spectroscopy (FTIR). PS@NiAlFe-LDH was evaluated for the elimination of Cd^{2+} ions from an aqueous solution in a batch system under different experimental conditions (initials solution pH, PS@NiAlFe-LDH dosage, initial Cd^{2+} concentration, agitation speed, and contact time). The isotherms, kinetics, adsorption mechanisms, and reusability were also investigated.

2. Materials and Methods

Styrofoam, Sodium carbonate [Na_2CO_3], Sodium dodecyl sulfate [$NaC_{12}H_{25}SO_4$], and potassium persulfate (KPS) [$K_2S_2O_8$] were used for the preparation of polystyrene nanoparticles. Nickel nitrate [$Ni(NO_3)_2$], ferric nitrate [$Fe(NO_3)_3$], and aluminum nitrate nonahydrate [$Al(NO_3)_3 \cdot 9H_2O$] used for LDH preparation.

2.1 Synthesis of Adsorbent

2.1.1 Synthesis of PS nanospheres

PS nanosheres were prepared using styrene, which was recovered from recycling Styrofoam waste by the thermal depolymerization of styrofoam waste, as a monomer. To reduce the volume and increase the density of the styrofoam, it was dissolved in acetone; releasing all the trapped air in Styrofoam [Figure 1(a)]. The mixture was heated to evaporate all the acetone, leaving a solid plastic material (polystyrene). Polystyrene was added to a distillation apparatus to produce a translucent yellow liquid (crude styrene) [Figure 1(b)]. A second distillation was conducted to obtain pure styrene by collecting it at a temperature (145 °C - 150 °C), since styrene distils above 145 °C (Figure 1(c)). The product was stored in a cool, dark place to prevent the auto-polymerization of styrene monomer into polystyrene. PS nanospheres were prepared,

using the previously prepared monomer styrene via emulsion polymerization. 0.0996 g of Na_2CO_3 and 0.1989 g of SDS were added to 250 mL of deionized water, and the mixture was purged with N_2 gas for 30 min. Then 30 mL of previously prepared styrene was added, and the mixture was stirred at 60 °C for 30 minutes. The polymerization was initiated by adding a KPS solution prepared by dissolving 0.9326 g of KPS in 15 mL of deionized water. The mixture was then stirred at 80 °C for 24 hours. A white powder (PS nanospheres) was collected by centrifugation, washed with methanol, and dried at 80 °C for 24 hrs. Figure 2 shows a schematic illustration of the preparation of PS nanospheres.

2.1.2 Synthesis of PS@NiAlFe-LDH

PS@NiFeAl-LDH was prepared by in-situ coprecipitation of metal ions on the PS core. PS nanosphers were added to distilled water, and the pH was adjusted to 9±0.1 by adding a dropwise 0.1 M NaOH solution. The PS nanosphere solution was stirred for 30 minutes. Metal salts solutions [$Ni(NO_3)_2$, $Al(NO_3)_3 \cdot 9H_2O$, and $Fe(NO_3)_3$] with Ni/(Al+Fe) molar ratio of 2:1 were added to the PS nanosphere solution with different LDH:PS ratios of (1:1, 2:1, and 3:1) while maintaining the pH at 9±0.1. The mixture was aged at 80 °C for 24 h. The product was centrifuged and then washed three times with deionized water. The precipitate was dried in a drying oven at 70 °C for 24 h. Figure 3 shows the steps of NiAlFe-LDH preparation.

2.2. Batch Experiments

The batch experiments were conducted to investigate the influence of adsorption parameters, including pH, initial Cd^{2+} concentration, PS@NiAlFe-LDH dose, agitation speed, and contact time. The samples were analyzed by atomic absorption spectroscopy (AAS), and the efficiency (E) of Cd^{2+} removal was determined using Equation (1) [24]. The amount of Cd^{2+} adsorbed per unit mass (q_e, mg/g) or adsorption capacity can be calculated by Equation (2) [25,26]:

$$E\ (\%) = \frac{C_i - C_e}{C_i} * 100 \qquad (1)$$

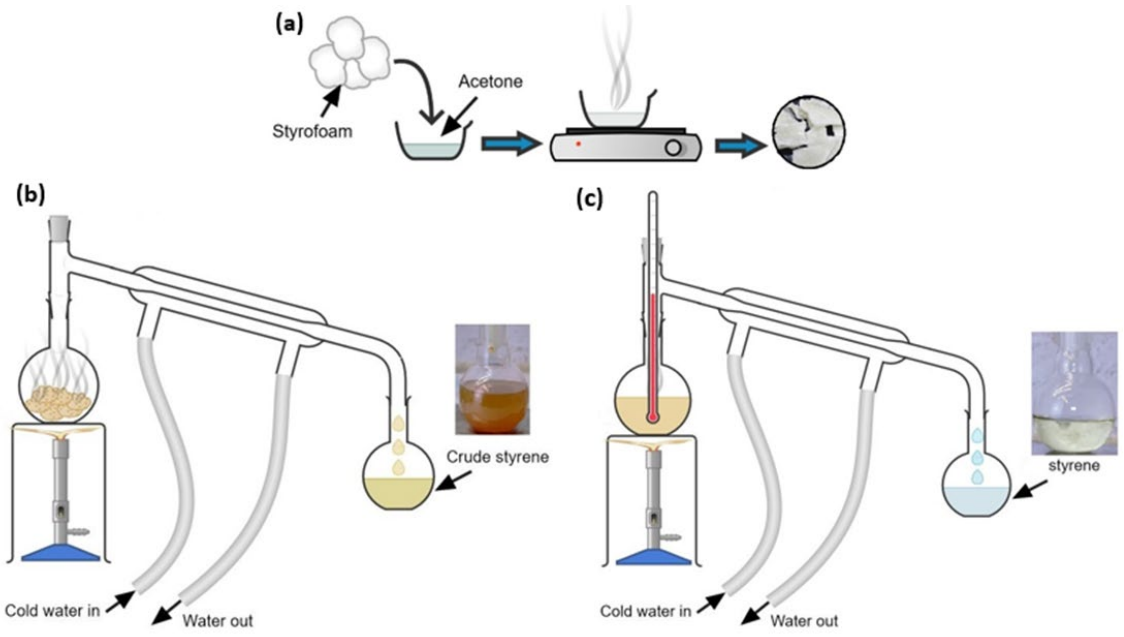

Figure 1. Schematic illustration of styrene preparation.

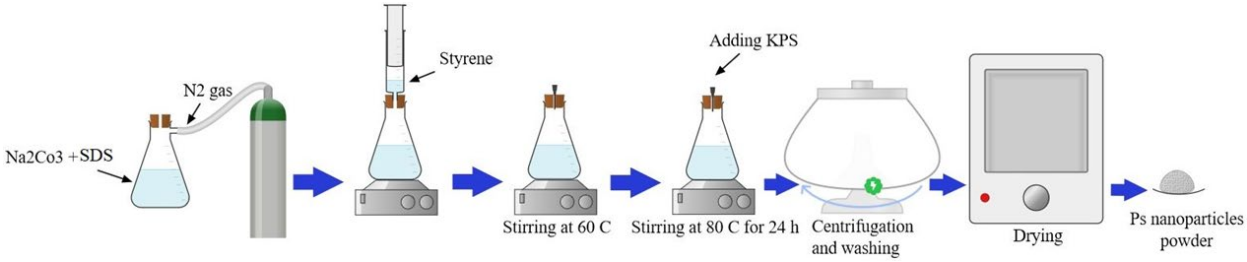

Figure 2. Schematic illustration of PS nanoshperes preparation.

$$q_e = \frac{(C_i - C_e)}{W} * V \quad (2)$$

Where C_i and C_e are the original (initial) and equilibrium concentration of Cd^{2+} (mg/L), respectively, and W is the mass of PS@NiAlFe-LDH (g).

2.3. Adsorption Isotherms and Kinetics

To describe the interactions between Cd^{2+} ions in solution and PS@NiAlFe-LDH, Langmuir and Freundlich adsorption isotherms were used. Non-linear optimization of Langmuir (Equation (3)] and Freundlich (Equation (4)) models was used to analyze the isothermal data [27,28]:

$$q_e = \frac{q_m\, k_L\, C_e}{1 + k_L\, C_e} \quad (3)$$

$$q_e = k_f\, C_e^{\frac{1}{n}} \quad (4)$$

Where q_e and q_m are the equilibrium and maximum adsorption capacities (mg/g), respectively. k_L is the Langmuir model constant, k_f and n are Freundlich model constants.

Pseudo-first-order (PFO) and pseudo-second-order (PSO) kinetic models were utilized to describe the rate of retention or release of a Cd^{2+} from an aqueous solution to the solid-phase interface. PFO (Equation (5)) and PSO (Equation (6)) models can be stated by [29]:

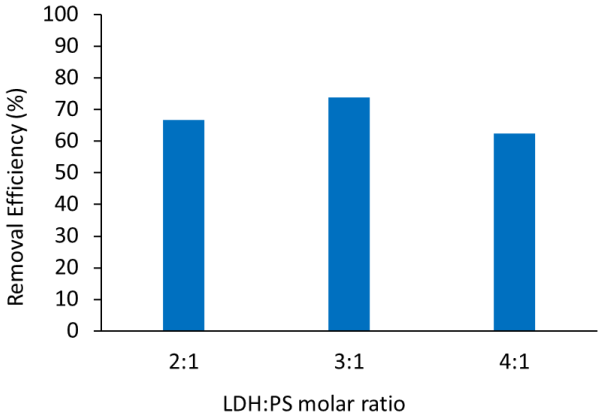

Figure 4. Removal efficiencies for PS@NiAlFe-LDH nanocomposite preparation ratios.

$$\ln(q_e - q_t) = \ln(q_e) - k_1\, t \quad (5)$$

$$\frac{t}{q_t} = \frac{1}{k_2\, {q_e}^2} + \frac{t}{q_e} \quad (6)$$

Where q_e and q_t, mg/g, are the amount of cadmium adsorbed at equilibrium and at time, t, min, respectively, k_1 and k_2 are the PFO and PSO constants of the equilibrium rate (min^{-1}), respectively.

Intra-particle-diffusion (Equation (7)) was applied to explore the mechanism of Cd^{2+} adsorption on PS@NiAlFe-LDH, which is described by the mode of diffusion or transportation of Cd^{2+} from the solution onto the solid phase [30,31]:

$$q_t = k_i\, t^{0.5} + C \quad (7)$$

Where q_t is the quantity of Cd^{2+} adsorbed (mg/g) at time t (min.), k_i is the IDF rate constant ($mg/g.min^{0.5}$), and C is the intercept related to the thickness of the boundary layer (mg/g).

3. Results and Discussion

3.1 PS@NiAlFe-LDH Synthesis

PS@NiAlFe-LDH was synthesized with LDH:PS ratios of 2:1, 3:1, and 4:1. The prepared nanocomposites were tested for Cd^{2+} adsorption as shown in Figure 4. It was found that a 3:1 ratio resulted in the highest removal efficiency, thus it was selected for the synthesis of PS@NiAlFe-LDH nanocomposite.

3.2 Characterizations

3.2.1 SEM and TEM analysis

The morphology of PS@NiFeAl-LDH and PS nanosphers was examined by SEM and TEM, as shown in Figure 5. Figure 5(a) indicates that PS nanospheres were successfully synthesized. Figure 2(b) shows that NiFeAl-LDH were successfully synthesized with a platelet morphology and uniformly attached to the surface of PS Nanospheres, which corresponds to the TEM image (Figure 5 (c)), and confirms the successful preparation of PS@NiFeAl-LDH

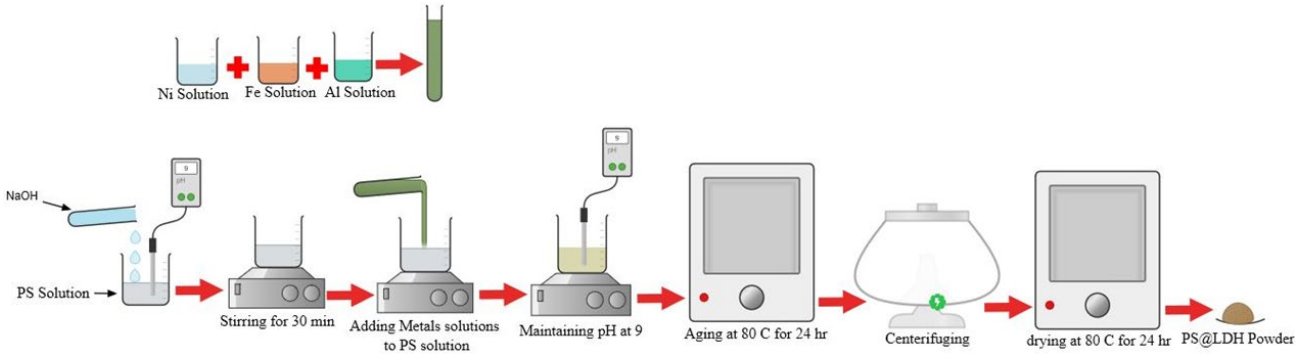

Figure 3. Diagram of the preparation of PS@NiAlFe-LDH nanocomposite.

nanocomposite. SEM also analyzed the morphology of PS@NiFeAl-LDH after the adsorption of Cd^{2+} ions (Figure 5(d)). It can be observed that Cd^{2+} ions did not alter the structural features of PS@NiFeAl-LDH nanocomposite, confirming the stability of PS@NiFeAl-LDH in acidic environments [32].

An analysis of the elemental content of PS@NiFeAl-LDH before and after Cd^{2+} adsorption was conducted with Energy Dispersive Spectra (EDS) maps. Figure 6(a) shows that PS@NiFeAl-LDH contained a large amount of carbon from the surface of PS nanospheres as well as nickel, iron, and aluminium from the NiFeAl-LDH. Figure 6(b) shows an additional element (Cadmium), which confirms the adsorption of Cd^{2} onto the PS@NiFeAl-LDH@ nanocomposite.

3.2.2. XRD analysis

The crystallinity and crystal structure of PS nanospheres and PS@NiFeAl-LDH nanocomposite was analyzed by XRD. Figure 7(1) showed the XRD patterns of PS nanospheres and PS@NiFeAl-LDH nanocomposite. A board peak can be observed at 23.02º-25º (*d*-spacing = 2.8577 Å), which is the most dominant feature indicating the amorphous nature of PS nanospheres, as well as their nano-size [33]. The PS@NiFeAl-LDH nanocomposite exhibits peaks at 12.03° (*d*-spacing = 7.26 Å), 29.6775° (*d*-spacing = 3.013 Å), and 32.125 ° (*d*-spacing = 2.783 Å), corresponding to the (104) plane, indicating a spherical polycrystalline structure that is predominant in the crystalline structure. A peak at 39.225º (*d*-spacing = 2.295 Å) corresponding to (006) plane indicates the presence of NiAlFe-LDH shell. Sharp and intense peaks with a reduced d-spacing at increasing 2θº indicate that the material's crystals are uniformly arranged. The peak of the (300) plane at 63.725° (*d*-spacing = 1.485 Å) reflects the existence of three metal cations in the host layer [34]. Creystalline size for PS@NiFeAl-LDH nanocomposite was calculated using Scherrer equation and it was found to be equal to 59.86 nm.

3.2.3 FTIR analysis

FTIR spectra of PS and PS@NiAlFe-LDH (before and after Cd^{2+} adsorption) are shown in Figure 7(2). The spectrum of PS nanospheres have a C–H aromatic stretching peak at 3028.66 cm^{-1}, a C–H aliphatic stretching peak at 2920.66 cm^{-1}, a

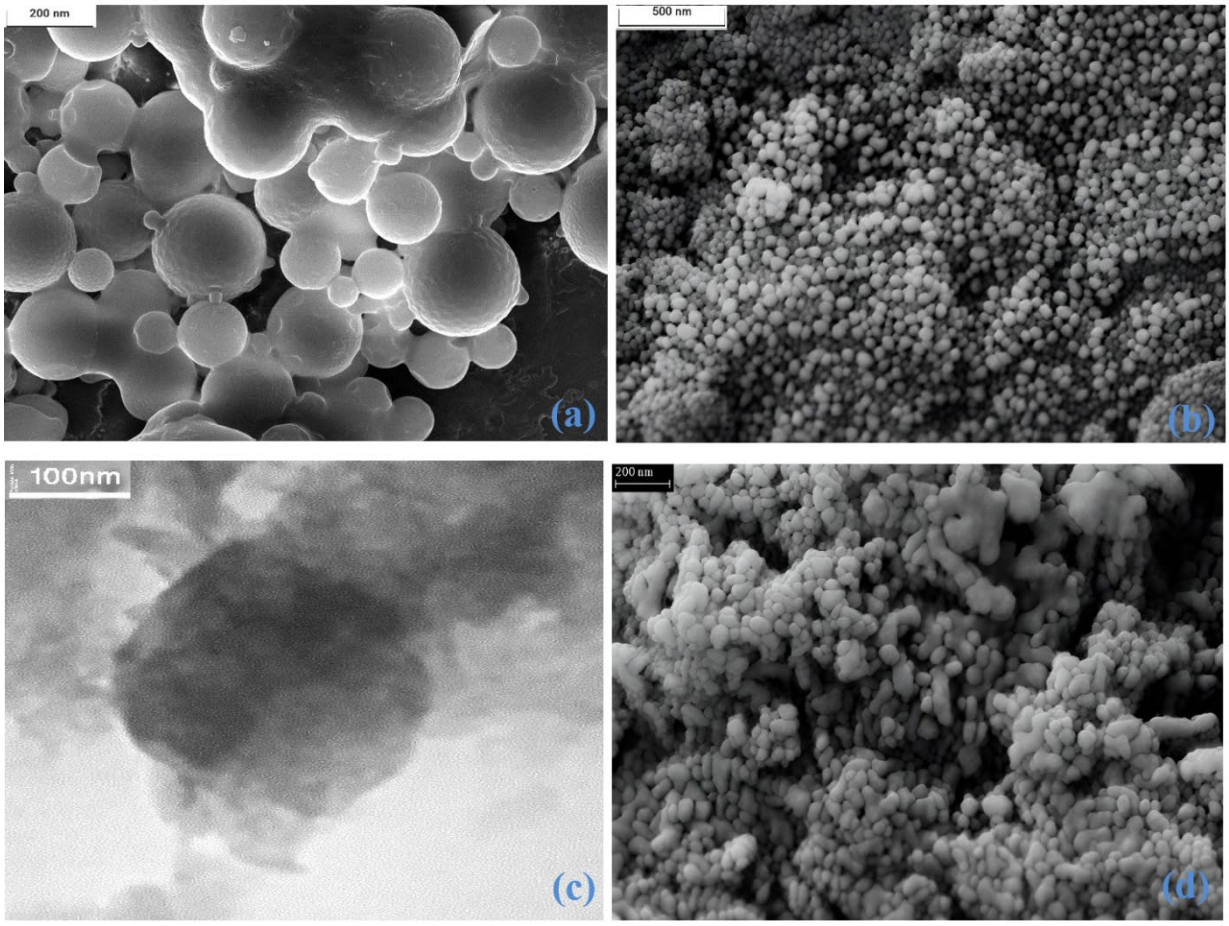

Figure 5. (a) SEM of PS nanospheres; (b) SEM of PS@NiFeAl-LDH nanocomposite; (c) TEM of PS@NiFeAl-LDH nanocomposite; and (d) SEM of PS@NiFeAl-LDH nanocomposite after Cd^{+2} adsorption.

C=C aromatic stretching at 1603.52 cm^{-1} and 1452.14 cm^{-1} indicating the presence of a benzene ring, and an aromatic C–H bending peak at 755.959 cm^{-1}, a characteristic peaks confirm the successful preparation of PS nanosphers [35,36]. In PS@ NiAlFe-LDH spectrum, new peaks appear (a strong broad O–H stretching peak at 3439.42 cm^{-1} and H–O–H bending peak at 1630 cm^{-1}, which are due to the O–H groups vibration in water molecules between the layers and/or the H bonds [37,38], a M–O/M–OH (M represents Ni, Al, or Fe) peak at 431.01 cm^{-1}, and at 1122 cm^{-1} related to the interlayer NO_3 ions stretching vibration) without a significant change in the PS nanosphers spectrum peaks, indicating the formation of NiAlFe-LDH shell on PS core. PS@ NiAlFe-LDH was also analyzed after the adsorption of Cd^{2+}; a change in the peaks appears due to the adsorption of Cd^{2+}. The O–H stretching and H–O–H bending peaks were reduced due to Cd^{2+} binding. A shift in the M-O/M-OH peak and a new peak appear at 618.07 cm^{-1} due to the Formation of Cd–O or Cd–OH after adsorption [39]. These changes indicate the adsorption of Cd^{2+} on PS@ NiAlFe-LDH nanocomposite.

3.2.4 BET analysis

The N_2 adsorption-desorption isotherm (Figure 8) was conducted to obtain the porous structure and pore size distribution of PS@NiAlFe-LDH. As stated by the International-Union-of-Pure-and-Applied-Chemistry (IUPAC) classes of adsorption isotherms, PS@NiAlFe-LDH isotherm is (Type IV) adsorption isotherm with (H3-type) hysteresis-loop due to the aggregation of platelet particles, which indicates a mesoporous structure with slit-shaped pores and extensive distribution of pore size ranging from 1.52 to 52.22 nm, resulting in rapid adsorption [40]. BET theory was used to determine the specific surface area, average pore volume, and pore diameter, which are listed in Table 1. The surface area of PS@NiAlFe-LDH is higher than that of PS, which indicates that coating PS nanosphers with a shell of NiAlFe-LDH increased their surface area, resulting in greater adsorption capacity.

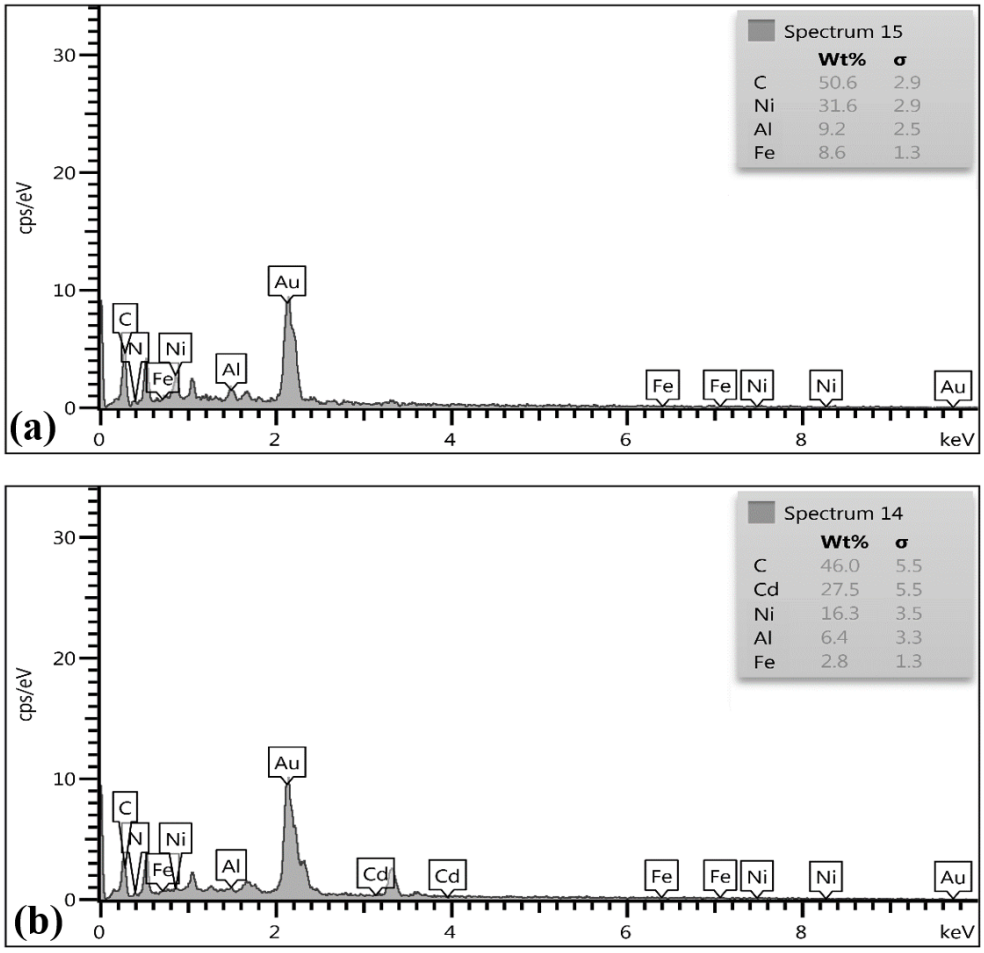

Figure 6. EDS examination of (a) PS@NiFeAl-LDH nanocomposite and (b) PS@NiFeAl-LDH after Cd^{2+} adsorption.

3.3. Influence and Optimization of Adsorption Parameters

3.3.1. Effect of pH

The initial pH plays an essential role in determining the adsorption capacity of adsorbents. The pH significantly affects Cadmium (Cd) adsorption by altering Cd's speciation in solution and the charge of the PS@NiAlFe-LDH surface [41]. The impact of pH on the removal efficiency of Cd^{2+} was explored a pH range (2-8). The efficiency of Cd^{2+} removal was increased with raising pH from 2 to 8, with maximum efficiency at pH of 6, while it decreases when pH>6 as shown in Figure 9(a). This behaviour was associated with the surface chemistry of the PS@NiAlFe-LDH composite, as the pH can modify the adsorbent surface. The point of zero charges (pH_{PZC}) for PS@NiAlFe-LDH was calculated by using the salt addition method, and it was found to be 4.43, as shown in Figure 9(b). When pH < pH_{PZC}, PS@NiAlFe-LDH develop a positive charge, resulting in an electrostatic repulsion between Cd^{2+} ions and PS@NiAlFe-LDH as well as H^+ ions competing on the active sites, leading to a decrease in Cd^{2+} adsorption. When pH > pH_{PZC}, PS@NiAlFe-LDH surface became negatively charged and thus increases the electrostatic attraction between Cd^{2+} ions and PS@NiAlFe-LDH, resulting in an increased adsorption of Cd^{2+} ions. Increasing the pH to more than 8 results in the precipitation of Cd as $Cd(OH)_2$; thus, an increase in removal efficiency can be observed, not due to actual adsorption, but rather due to precipitation [24]. The mechanism of adsorption is highly influenced by changes in pH. At low pH, the dominating process is ion exchange with H^+ and metals in the LDH (forming inner sphere complexes). While at high pH, Cd^{2+} adsorption is accomplished by the release of H^+ ions. Thus, a pH higher than pH_{PZC} was favourable in this study as the negatively charged sites increased,

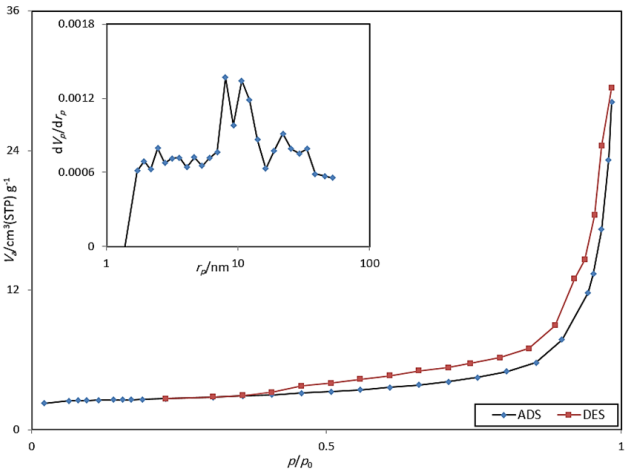

Figure 8. BET-BJH analysis for PS nanospheres and PS@NiAlFe-LDH nanocomposite.

Table 1. BET-BJH analysis for PS nanospheres and PS@NiAlFe-LDH nanocomposite.

Material	Surface area, m^2/g	Average pore volume, cm^3/g	Average pore diameter, nm
PS	15.304	0.014	5.97
PS@NiAlFe-LDH	159.35	0.031	18.97

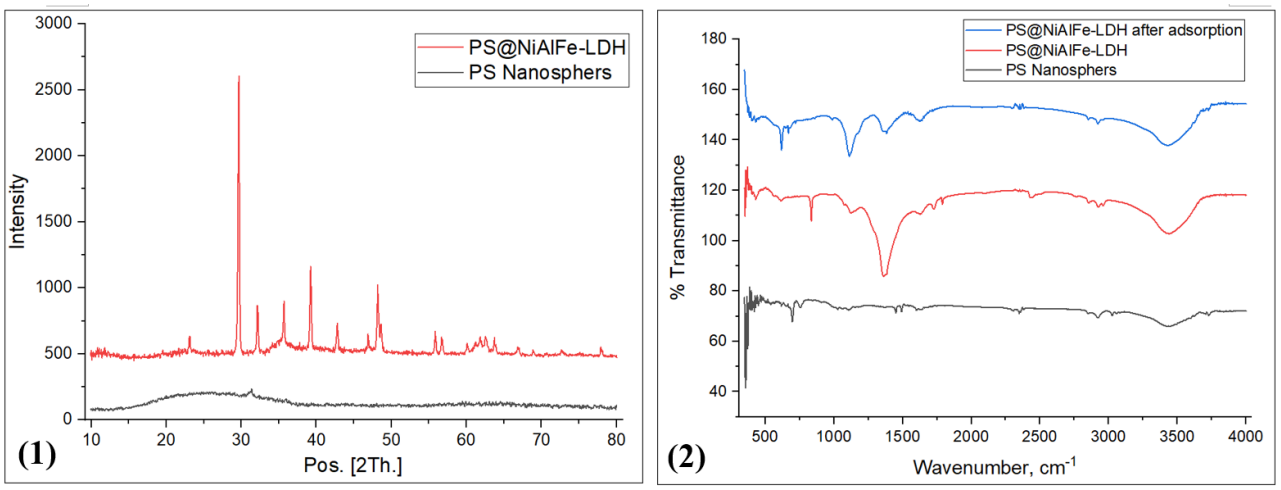

Figure 7. (1) XRD patterns for PS and PS@NiFeAl-LDH; (2) FTIR of PS, PS@NiAlFe-LDH, and PS@NiAlFe-LDH after Cd^{2+}.

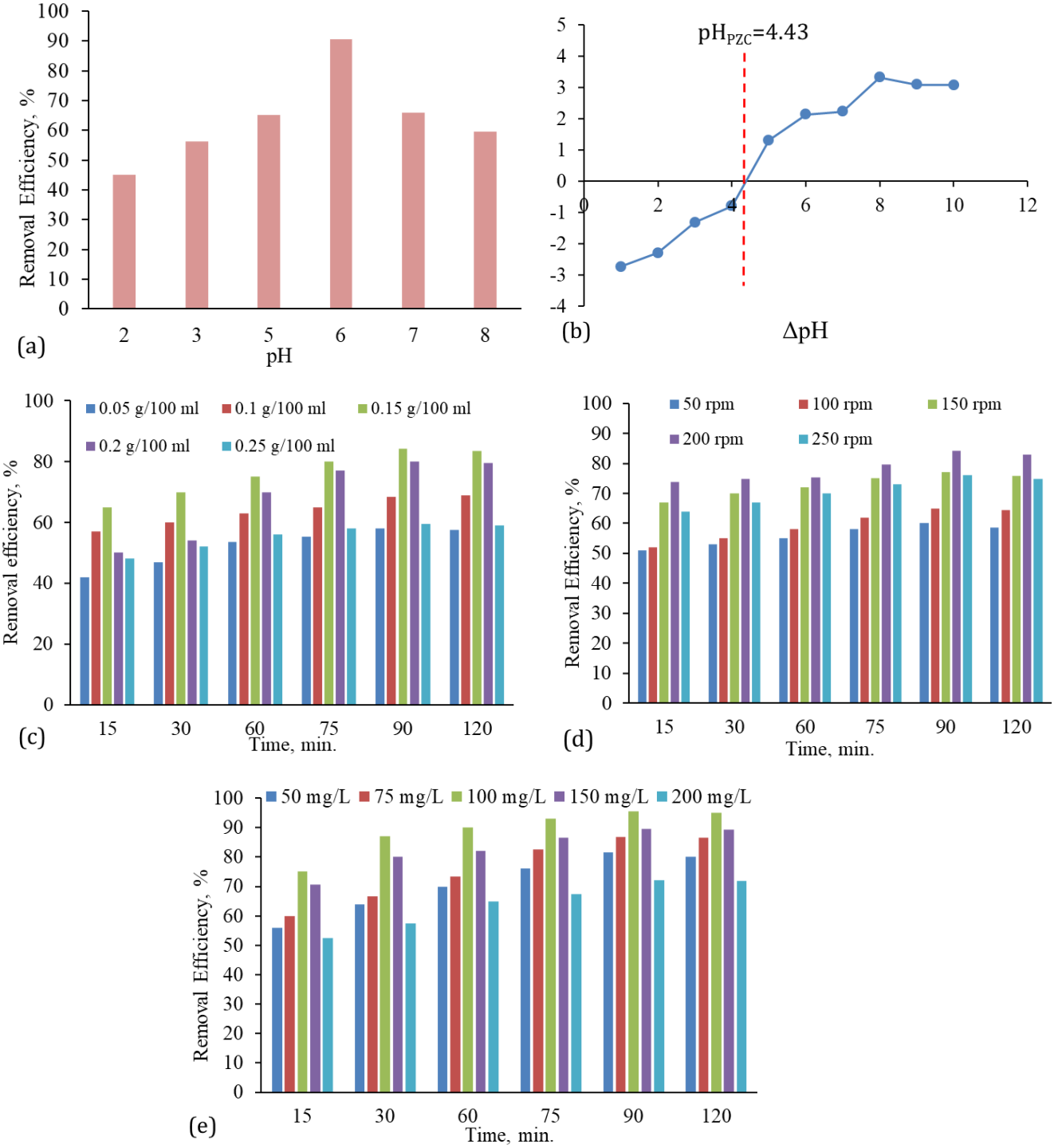

Figure 9. The effect of parameters on Cd^{2+} adsorption: (a) pH [at conditions of 0.15 mg adsorbent/100 mL, 150 rpm, 150 mg/L initial concentration and 90 min contact time]; (b) pH_{PZC} for PS@NiAlFe-LDH; (c) Adsorbent dosage [at conditions of pH of 6, 150 rpm and 150 mg/L initial concentration]; (d) Shaking speed [at conditions of pH of 6, 0.15 mg adsorbent/100 mL and 150 mg/L initial concentration]; and (e) Initial concentration [at conditions of pH of 6, 0.15 mg adsorbent/100 mL and 200 rpm].

which is favoured for the adsorption of positively charged Cd^{2+} ions.

3.3.2. Effect of NiAlFe-LDH@PS dosage

The dose of adsorbent can also influence the removal of contaminants. The influence of adsorbent dosage was investigated at various dosages ranging from 0.05 to 0.25 g of PS@NiAlFe-LDH/100 mL (Figure 9(c)). Increasing PS@NiAlFe-LDH dosage increase the overall percentage of cd removed due to providing a greater surface area and more active sites for the cadmium ions to bind [42], and increasing of the concentration gradient between the liquid and solid phases, which speeds up the mass transfer of Cd ions to PS@NiAlFe-LDH surface, thus the removal efficiency increased as PS@ increased reaching a maximum removal at a dose of 0.15 g/100 mL. while increasing PS@NiAlFe-LDH more than 0.15 g/100 mL resulted in reducing the adsorption capacity as all Cd^{2+} were adsorbed and many of the active sites remain unsaturated as the available Cd^{2+} ions were distributed across a larger number of adsorption sites [43]. This reduces the amount of Cd adsorbed per gram of the adsorbent, resulting in a decrease in the adsorption capacity. Thus, a PS@NiAlFe-LDH dose of 0.15 g/100 mL was selected as the optimum adsorbent dosage.

3.3.3. Effect of shaking speed

Shaking speed is an important factor in the adsorption of Cd^{2+} ions that impacts the contact between Cd^{2+} ions and PS@NiAlFe-LDH and affects the distribution of Cd^{2+} ions in solution, thus affecting the adsorption kinetics. The effect of shaking speed on the adsorption of Cd ions was investigated at a range of 50 – 250 rpm (Figure 9(d)). The efficiency increased with increasing the shaking speed, reaching its maximum at 200 rpm. At low shaking speeds, the PS@NiAlFe-LDH particles were not distributed enough to provide the active sites, and a thick diffusion layer can form around PS@NiAlFe-LDH particles, limiting the rate at which Cd^{2+} ions reach the binding sites. As the shaking speed increases, the thickness of the boundary layer surrounding the PS@NiAlFe-LDH particle decreases, thereby improving mass transfer and increasing the adsorption rate. It was observed that increasing the shaking speed further reduces the removal efficiency of Cd^{2}, as the added energy can break the bonds that have already formed between the Cd ions and the PS@NiAlFe-LDH surface, thereby reducing the overall removal efficiency. Thus, a shaking speed of 200 rpm was selected as the optimum speed for the adsorption of Cd^{2+}.

3.3.4. Effect of initial Cd^{2+} concentration and contact time

The initial concentration of Cd^{2+} ions affects the driving force for mass transfer and the frequency of collisions between Cd molecules and PS@NiAlFe-LDH active sites [12]. The influence of initial Cd^{2+} concentration was investigated over a range (50-150) mg/L (Figure 9(e)). It was observed that the removal of Cd^{2+} ions increased with increasing the initial concentration, reaching a maximum removal when the initial concentration was 100 mg/L. Increasing the initial concentration provides a stronger concentration gradient, increasing the driving force for Cd^{2+} ions to move from the solution to the PS@NiAlFe-LDH surface and onto the active sites as well as increasing Cd^{2+} molecules present in the solution, which results in more frequent collisions with the PS@NiAlFe-LDH surface, increasing the rate of adsorption [44]. However, increasing the initial concentration more than 100 mg/L resulted in decreased removal efficiency as the available adsorption sites on PS@NiAlFe-LDH become saturated and even if the total amount of Cd^{2+} ions adsorbed increase, the percentage of the total Cd^{2+} ions removed from the solution decrease because there is not enough adsorbent to handle the large quantity of Cd^{2+} ions, thus an optimum initial concentration of 100 mg/L was selected for the adsorption of Cd^{2+} ions on PS@NiAlFe-LDH.

The adsorption parameters were tested at various periods, ranging from 15 to 120 minutes. Initially, the adsorption capacity increased rapidly because of the abundance of active sites on the PS@NiAlFe-LDH surface for Cd^{2+} ions to attach to. Subsequently, the rate of adsorption slowed down as more Cd^{2+} molecules adsorb, and the number of available sites decreased, leading to a slower rate of adsorption until equilibrium was reached at 90 min when the PS@NiAlFe-LDH surface is saturated. The rate of adsorption equals the rate of desorption, resulting in a nearly constant removal efficiency [26]. The optimum conditions for Cd^{2+} adsorption on PS@NiAlFe-LDH are listed in Table 2.

Table 2. Optimum factors for the adsorption of Cd^{2+} on PS@NiAlFe-LDH.

Parameter	Optimum value
pH	6
Initial Cd^{+2} concentration, mg/L	100
PS@NiAlFe-LDH dose, g/100 mL	0.15
Shaking speed, rpm	200
Contact time, min	90

3.4. Adsorption Isotherms

Isotherm models play an essential role in predicting the relationship between the amount of Cd^{2+} adsorbed and its concentration at equilibrium. The results of Langmuir and Freundlich's non-linear analysis are shown in Figure 10, while the constants and variables are present in Table 3. The Langmuir isotherm described the adsorption of Cd^{2+} ions on PS@NiFeAl-LDH, yielding a higher correlation coefficient (R^2) and maximum capacity of 227.273 mg/g, indicating a homogenous PS@ surface with a finite number of identical sites and a monolayer adsorption with adsorption site [27]. The value of the separation factor (R_L) was obtained for all initial concentrations and it was found to be less the 1 and higher than 0, for all initial concentration, indicating a favorable adsorption of Cd^{2+} ions on PS@NiFeAl-LDH nanocomposite [45].

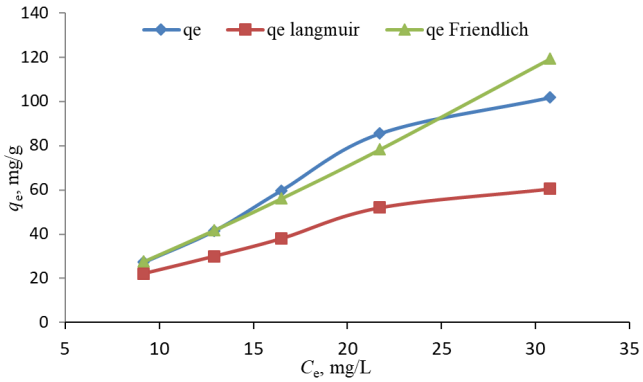

Figure 10. Isotherm models for the adsorption of Cd^{2+}.

3.5. Kinetics of Adsorption

To study the kinetics of cadmium Cd^{2+} ions adsorption on PS@NiAlFe-LDH nanocomposite, the pseudo-first-order (PFO), and pseudo-second-order (PSO) models were utilized. Figure 11(a,b) shows the fitted data for both models, while Table 4 represents the kinetic parameters and correlation coefficient (R^2). The kinetics of cadmium (Cd^{2+}) adsorption on PS@NiAlFe-LDH nanocomposite were described by the PSO model due to greater R^2 values, and the theoretical $q_{(e(model))}$ being closer to the experimental $q_{(e(exp.))}$ revealing that the rate-controlling step of Cd^{2+} adsorption was a chemical reaction, indicating a chemisorption process [46]. Cadmium reacts with functional groups on the surface of PS@NiAlFe-LDH nanocomposite (e.g., –OH, –COOH) through covalent bonds, resulting in the formation of surface complexes. This leads to stable and strong binding of cadmium on the surface of PS@NiAlFe-LDH nanocomposite and a difficult re-extraction of Cd^{2+} ions (low desorption). The diffusion mechanism of Cd^{2+} ions was evaluated by the intra-particle-diffusion kinetic model (IPD); Figure 11(c) shows a three-step adsorption process. The first was the film diffusion stage, in which Cd^{2+} ions were transferred from the bulk solution to the liquid film around PS@NiAlFe-LDH nanocomposite by electrostatic attraction and took about 15 min. The adsorption capacity increased rapidly due to the presence of numerous active sites. The second stage was the internal diffusion, in which Cd^{2+} ions transferred to the pores of PS@NiAlFe-LDH nanocomposite and adsorbed on the active sites and took about 60 min. The adsorption rate slowed down compared to the first stage due to the saturation of the

Table 3. Isotherm parameters for the adsorption of Cd^{2+}.

Isotherm	Parameter	Value
Langmuir	q_{max}	227.273
	K_L	0.012
	R^2	0.9941
	R_L (Co=100 mg/L)	0.46
	SSR	268.93
	X^2	0.231
Freundlich	K_f	29.65
	$\frac{1}{n}$	1.21
	R^2	0.922
	SSR	984.1
	X^2	12.4

surface active sites. Eventually, Cd^{2+} ions settle on the active sites (functional groups such as –OH, –COOH, or sites with positive or negative charges) and the adsorption reaches equilibrium in about 15 minutes. The intra-particle diffusion is the rate-limiting step [47]. Table 5 represents the parameters of the IPD model. Table 6 compares the adsorption capacity of PS@NiAlFe-LDH nanocomposite with those reported in other studies on Cd^{2+} adsorption.

3.6. Adsorption Mechanism

Coating PS nanospheres with a shell of NiAlFe-LDH enhanced their properties, such as surface area and pore volume. As the pH of the solution was greater than pH_{PZC} of PS@NiAlFe-LDH, the hydroxyl and carboxyl groups ratio on the PS@NiAlFe-LDH surface increased in the form of -COOH and -O- due to the dissociation of oxygen-containing groups on the PS@NiAlFe-

Table 4. Parameters for PFO and PSO models for the adsorption of Cd^{2+} ions on PS@NiAlFe-LDH nanocomposite.

Kinetic	Parameter	Value				
		C_o = 50 mg/L	C_o = 75 mg/L	C_o = 100 mg/L	C_o = 150 mg/L	C_o = 200 mg/L
PFO	$q_{e(Exp.)}$	27.24	43.67	63.68	89.48	96.15
	$q_{e(model)}$	18.48	36.86	33.18	63.77	95.6
	R^2	0.9588	0.9599	0.9491	0.9451	0.9315
	K_1	0.0301	0.038	0.039	0.048	0.048
PSO	$q_{e(Exp.)}$	27.24	43.67	63.68	89.48	96.15
	$q_{e(model)}$	27.7	45.045	64.516	90.91	99.01
	R^2	0.9914	0.9886	0.9985	0.9975	0.9942
	K_2	0.0063	0.0034	0.0057	0.0035	0.0019

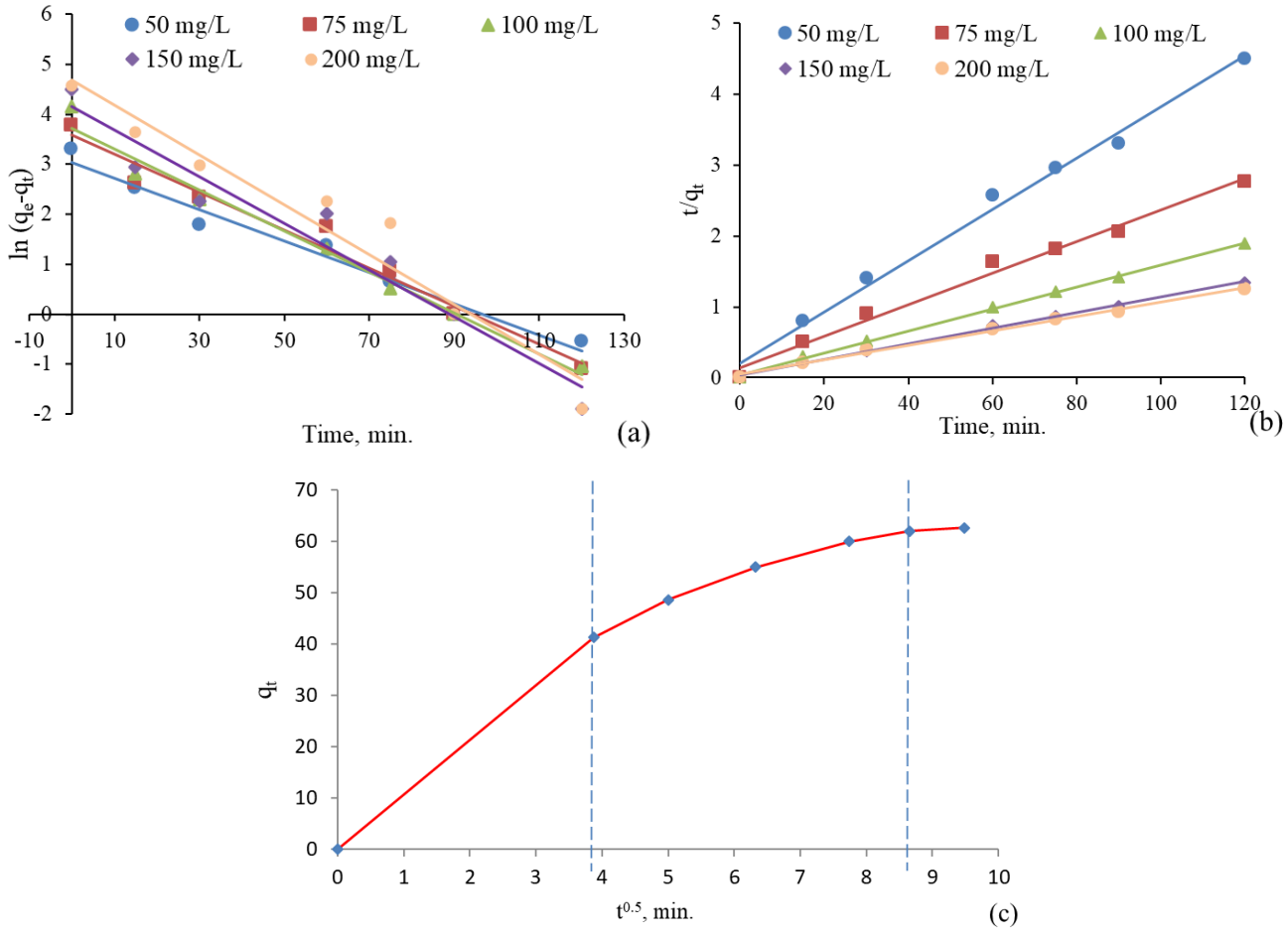

Figure 11. Adsorption Kinetics for Cd^{2+} ions (a) PFO; (b) PSO; and (c) IPD.

LDH surface, increasing the electrostatic attraction between Cd^{2+} ions and the PS@NiAlFe-LDH surface. Some of Cd^{2+} ions diffused to the PS@NiAlFe-LDH pores, which undergo reactions with the functional groups, such as -OH, =O-, and -COOH, to form surface complexes [63]. This can be observed in the FTIR analysis of PS@NiAlFe-LDH (Figure 7(2)) as the hydroxyl group (-OH vibrations) peak at 3426 cm^{-1} was reduced, and -COOH vibration (C=O stretching) at 1726.9 cm^{-1} shifted to 1629.55 cm^{-1}, proving the formation of complexes. As a result, the adsorption of Cd^{2+} ions on PS@NiAlFe-LDH nanocomposite was chemisorption, and the rate of adsorption was primarily controlled by the chemical reaction between Cd^{2+} ions and PS@NiAlFe-LDH surface [31]. Thus, Cd^{2+} ions were adsorbed through three mechanisms: electrostatic force interaction, interaction with oxygen-containing functional groups, and complexation reactions. Figure 12 represents an illustration of the adsorption mechanism of Cd^{2+} ion on PS@NiAlFe-LDH nanocomposite.

3.7. Reusability of PS@NiAlFe-LDH Nanocomposite and Desorption of Cadmium Ions

To evaluate PS@NiAlFe-LDH reusability, six successive regeneration cycles (adsorption-desorption) were conducted. 500 mg of PS@NiAlFe-LDH were mixed with 100 mL of 0.5 M HNO_3. The mixture was stirred for 180 minutes, then centrifuged, washed, and oven-dried. The regeneration process was repeated six times. Figure 13 shows the removal efficiency for each cycle, calculated using Equation (1). The removal efficiency of Cd^{2+} decreased to 57.56% after six regeneration cycles. This reduction was likely due to structural damage caused by exfoliation resulting from exposure to the acid solution [64]. The decrease in efficiency can also be due to the loss of PS@NiAlFe-LDH [65]. These results demonstrate that the PS@NiAlFe-LDH nanocomposite exhibits significant recyclability, indicating that it can be an efficacious, sustainable, and cost-effective sorbent for Cd^{2+} removal from aqueous solutions.

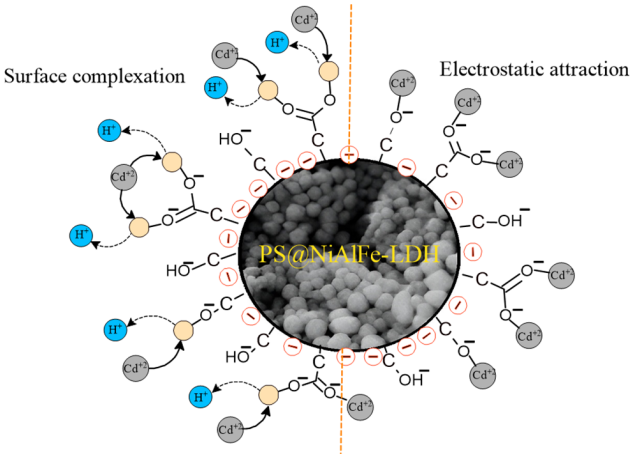

Figure 12. Schematic illustration of the adsorption mechanisms of Cd^{2+} on PS@NiAlFe-LDH.

Table 6. Comparison of the maximum adsorption capacity (q_{max}) of Cd^{2+} onto PS@NiAlFe-LDH with diverse adsorbents in previous studies.

Adsorbent	q_{max}, mg/g	Reference
Algae	18.19	[48]
Core–shell Fe_3O_4/polydopamine (Fe_3O_4@PDA)	21.58	[49]
Agave bagasse (AB)	28.5	[50]
Alang-alang grass (Imperata cylindrica)	4.43	[51]
Magnetic Oak wood ash/Graphene oxide (Ash/GO/Fe_3O_4)	43.66	[52]
Cassava root husk-derived biochar)-ZnO nanoparticles (CRHB-ZnO_3)	42.05	[53]
Cassava root husk-derived biochar (CRHB)	32.33	[53]
KOH-activated biochar (KOHBC)	29	[54]
Sulfhydryl attapulgite (SH-ATP)	21.5	[55]
BPAC@Al_2O_3@chitosan	46.9	[56]
MgAl-LDH/sodium hexametaphosphate (SHMP)	24.34	[57]
Red mud modified by manganese dioxide(MRM)	103.59	[58]
Succinic acid functionalized Fe_3O_4@AMPA	43	[59]
Humic acid with silica (HS)	6.25	[60]
Oxidized multi-walled carbon nanotubes (O-MWCNTS)	3.34	[61]
Fe_3O_4/SiO_2/ polyacrylamide (PAM)	13.22	[62]
Core – Shell PS@NiAlFe-LDH	227.273	Current Study

4. Conclusions

The present study showed that the prepared PS@NiAlFe-LDH nanocomposite utilizing Styrofoam waste was an efficient adsorbent for the removal of cadmium ions from aqueous solutions. It provides a clear chemical significance by demonstrating that coating polystyrene nanospheres with shell NiAlFe-LDH creates new active hydroxyl and layered sites that enhance Cd-binding efficiency, thus altering the surface chemistry and improving the adsorption performance significantly. Images of TEM and SEM showed the successful deposition of NiAlFe-LDH shell on PS nanosphers core. XRD and FTIR spectrums showed that PS@NiAlFe-LDH nanocomposite has a stable crystalline structure and offers high surface areas and functional groups capable of interacting with Cd^{2+} ions, which explains the high capacity and efficiency in adsorption. Spectral changes after adsorption (the formation of M–O and M–OH interactions) confirm the interaction of the functional groups with Cd^{2+} ions. Optimization experiment showed that the optimum removal of Cd^{2+} ions was at a pH of 6, a dose of 0.15 mg PS@NiAlFe-LDH /100 ml, Cd^{2+} initial concentration of 100 mg/L, shaking speed of 200 rpm and contact time of 90 minutes. Isotherm studies indicated that the Langmuir model fitted the experimental data better than the Freundlich model, with a maximum adsorption capacity of 227.273 mg/g, which is significantly higher than that of other similar absorbents. The pseudo-second-order kinetic model fitted the adsorption kinetic process, indicating chemisorption exists during the adsorption process. The IPD kinetic model revealed a three-stage adsorption process, with intra-particle diffusion as the rate-limiting step. Cd^{2+} ions were adsorbed on PS@NiAlFe-LDH nanocomposite via electrostatic force interaction, oxygen-containing functional groups, and complexation reactions. Furthermore, the PS@NiAlFe-LDH nanocomposite was easily regenerated and remained usable for six cycles, with a minimal reduction in removal efficiency of 36.86%. The study developed a new hybrid sorbent (PS@NiAlFe-LDH nanocomposite) with enhanced capacity, improved stability, and a clarified adsorption mechanism providing a clear framework for future heavy-metal remediation studiesis.

Declaration of Generative AI and AI-Assisted Technologies in the Writing Process

During the preparation of this work, the authors used Grammarly to assist with language refinement and grammar correction. After using this tool, the authors reviewed and edited the content as needed and took full responsibility for the published article.

Acknowledgment

This research work was not funded by any organization.

CRedit Author Statement

Author Contributions: Shahad A. Raheem: Conceptualization, Methodology, Investigation, Resources, and Data Curation, Writing; Ahmed A. Mohammed: Conceptualization, Formal Analysis, Review and Editing, Supervision. All authors have read and agreed to the published version of the manuscript.

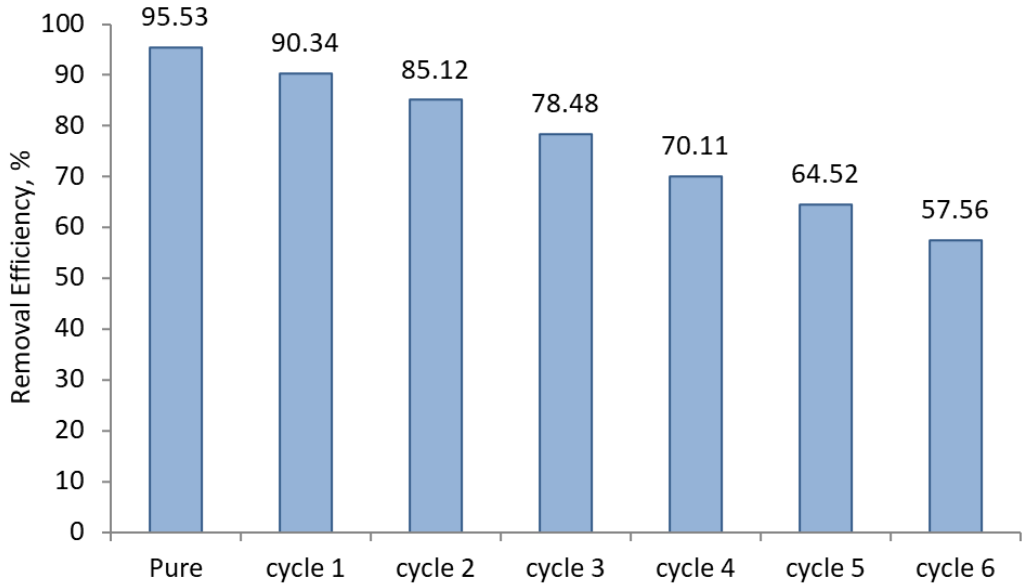

Figure 13. Regeneration of PS@NiAlFe-LDH (pH = 6, dosage= 0.15 g/100 mL, speed = 200, initial concentration = 100 mg/L, and contact time of 90 min.)

References

[1] Janighorban, M., Rasouli, N., Sohrabi, N., Ghaedi, M. (2020). Response Surface Methodology for Optimizing Cd(II) Adsorption onto a Novel Chemically Changed Nano Zn2Al-Layer Double Hydroxide. *Advanced Journal of Chemistry, Section A*, 3 (Special Issue), S701–S721. DOI: 10.22034/ajca.2020.106899.

[2] Pang, Y., Zhao, C., Li, Y., Li, Q., Bayongzhong, X., Peng, D., Huang, T. (2022). Cadmium adsorption performance and mechanism from aqueous solution using red mud modified with amorphous MnO2. *Scientific Reports*, 12(1), 1–18. DOI: 10.1038/s41598-022-08451-2.

[3] Desalegn, Y.M., Bekele, E.A., Olu, F.E. (2023). Optimization of Cd (II) removal from aqueous solution by natural hydroxyapatite/bentonite composite using response surface methodology. *Scientific Reports*, 13(1), 1–17. DOI: 10.1038/s41598-023-32413-x.

[4] Monika Mahajan, Gupta, P.K., Singh, A., Vaish, B., Singh, P., Kothari, R., Singh, R.P. (2022). A comprehensive study on aquatic chemistry, health risk and remediation techniques of cadmium in groundwater. *Science of The Total Environment*, 818, 151784. DOI: 10.1016/j.scitotenv.2021.151784.

[5] Mohammed, R.A., Abdulhasan, M.J., Raheem, S.A., Alwared, A.I., Mohammed, N.A., Kadhim, R.F., Al-Bayati, A.D.J. (2023). Optimization of Response Surface Methodology for Removal of Cadmium Ions from Wastewater using Low Cost Materials. *Journal of Ecological Engineering*, 24(8), 146–156. DOI: 10.12911/22998993/166371.

[6] Qiu, B., Tao, X., Wang, H., Li, W., Ding, X., Chu, H. (2021). Biochar as a low-cost adsorbent for aqueous heavy metal removal: A review. *Journal of Analytical and Applied Pyrolysis*, 155(February), 105081. DOI: 10.1016/j.jaap.2021.105081.

[7] Jasim, A.Q., Ajjam, S.K. (2024). Removal of heavy metal ions from wastewater using ion exchange resin in a batch process with kinetic isotherm. *South African Journal of Chemical Engineering*, 49(February), 43–54. DOI: 10.1016/j.sajce.2024.04.002.

[8] Kouzbour, S., Gourich, B., Gros, F., Vial, C., Stiriba, Y. (2022). A novel approach for removing cadmium from synthetic wet phosphoric acid using sulfide precipitation process operating in batch and continuous modes. *Minerals Engineering*, 187, 107809. DOI: 10.1016/j.mineng.2022.107809.

[9] Rahmadan, J., Parhusip, V., Palapa, N.R., Taher, T., Mohadi, R., Lesbani, A. (2021). ZnAl-Humic Acid Composite as Adsorbent of Cadmium (II) From Aqueous Solution. *Science and Technology Indonesia*. 6(4) 247-255. DOI: 10.26554/sti.2021.6.4.247-255

[10] Alnasrawi, F.A., Mohammed, A.A. (2023). Enhancement of Cd2+ removal on CuMgAl-layered double hydroxide/montmorillonite nanocomposite: Kinetic, isotherm, and thermodynamic studies. *Arabian Journal of Chemistry*, 16(2), 104471. DOI: 10.1016/j.arabjc.2022.104471.

[11] Silaen, L., Palapa, N.R., Juleanti, N., Normah, Mohadi, R., Elfita, Lesbani, A. (2020). Efficient Adsorption of Cadmium (II) on Zn/M3+ (M3+ = Al, Cr) AND Zn/M3+-[α-SiW12O40] Layered Double Hydroxides. *ARPN Journal of Engineering and Applied Sciences*, 15(18), 1967–1975.

[12] Mittal, J. (2021). Recent progress in the synthesis of Layered Double Hydroxides and their application for the adsorptive removal of dyes: A review. *Journal of Environmental Management*, 295(June), 113017. DOI: 10.1016/j.jenvman.2021.113017.

[13] Uttaravalli, A.N., Dinda, S., Gidla, B.R. (2020). Scientific and engineering aspects of potential applications of post-consumer (waste) expanded polystyrene : A review. *Process Safety and Environmental Protection*, 137, 140–148. DOI: 10.1016/j.psep.2020.02.023.

[14] Febriansya, A., Iskandar, Amalia, D., Indah, R.N., Widyaningsih, Y. (2024). Environmental implications of styrofoam waste and its utilization as lightweight fill material for embankment construction. *E3S Web of Conferences*, 479 DOI: 10.1051/e3sconf/202447907036.

[15] Bu, F., Huang, W., Xian, M., Zhang, X., Liang, F., Liu, X., Sun, X., Feng, D. (2022). Magnetic carboxyl-functionalized covalent organic frameworks for adsorption of quinolones with high capacities, fast kinetics and easy regeneration. *Journal of Cleaner Production*, 336, 130485. DOI: 10.1016/j.jclepro.2022.130485.

[16] Wen, Y., Xie, Z., Ye, H., Xue, S., Zhao, M., Liu, T., Shi, W. (2024). Conversion of waste polystyrene into porous adsorbents for efficient removal of hazardous pollutants: Adsorption properties and adsorption mechanism. *Journal of Environmental Chemical Engineering*, 12(6), 114440. DOI: 10.1016/j.jece.2024.114440.

[17] Hannun, R.M., Abdul Razzaq, A.H. (2022). Air Pollution Resulted from Coal, Oil and Gas Firing in Thermal Power Plants and Treatment: A Review. *IOP Conference Series: Earth and Environmental Science*, 1002(1) DOI: 10.1088/1755-1315/1002/1/012008.

[18] Soheilian, S., Jordan, B., Hatton, F.L. (2025). Impact of size and UV-ageing of polystyrene nanoparticles on copper(II) adsorption: kinetics and isotherms in aquatic environments. *Environmental Science Nano*, 12, 548–562. DOI: 10.1039/d4en00433g.

[19] Alyasi, H., Mackey, H.R., McKay, G. (2022). Comparison of Cadmium Adsorption from Water Using Same Source Chitosan and Nanochitosan: Is It Worthwhile to Go Nano? *Journal of Polymers and the Environment*, 30(7), 2727–2738. DOI: 10.1007/s10924-021-02344-7.

[20] Duan, L., Guo, C., Fan, J., Duan, Y., Qiu, P., Huang, P., Yan, J. (2023). A new method for preparing porous magnetic PS particles modified with EVA via a phase inversion emulsion procedure. *Colloid and Polymer Science*, 301(4), 293–302. DOI: 10.1007/s00396-023-05067-4.

[21] Xue, Z., Deng, X., Chen, Q., Zhao, J., Liang, H., Zhong, R., Yu, S., Kou, W., Li, C. (2025). Electrochemical Co-synthesis of graphene oxide and Mg(OH)2 for assembling hierarchical GO/Chitosan/Mg(OH)2 composites with enhanced Congo red adsorption. *Chemical Engineering Science*, 316, 122014. DOI: 10.1016/j.ces.2025.122014.

[22] Mohammed, A.A., Alnasrawi, F.A. (2024). Adsorption of Pb2+ ions by MgCuAl-layered double hydroxides@montmorillonite nanocomposite in batch and circulated fluidized bed system: Hydrodynamic and mass transfer studies. *Journal of Water Process Engineering*, 63(May), 105519. DOI: 10.1016/j.jwpe.2024.105519.

[23] Juleanti, N., Palapa, N.R., Taher, T., Hidayati, N., Putri, B.I., Lesbani, A. (2021). The Capability of Biochar-Based CaAl and MgAl Composite Materials as Adsorbent for Removal Cr (VI) in Aqueous Solution. *Science and Technology Indonesia*, 6(3), 196-203. DOI: 10.26554/sti.2021.6.3.196-203.

[24] Mohammed, A.A., Alnasrawi, F.A. (2024). Cadmium sequestration with MgCuAl-layered double hydroxide@montmorillonite nanocomposite in batch and circulated fluidized bed column experiments. *Desalination and Water Treatment*, 320(July), 100744. DOI: 10.1016/j.dwt.2024.100744.

[25] Kareem, S.L., Mohammed, A.A. (2020). Removal of Tetracycline from Wastewater Using Circulating Fluidized Bed. *Iraqi Journal of Chemical and Petroleum Engineering*, 21(3), 29–37. DOI: 10.31699/ijcpe.2020.3.4.

[26] Alnasrawi, F.A., Mohammed, A.A., Al-Musawi, T.J., Hussein, N.M. (2024). The efficient elimination of lead ions from aqueous solution using MgCuAl-Layered double hydroxides@montmorillonite composite: A kinetic, isotherm and statistical analysis. *Results in Surfaces and Interfaces*, 16, 100260. DOI: 10.1016/j.rsurfi.2024.100260.

[27] Mohammed, A.A., Ali, D.K. (2023). Bentonite-layered double hydroxide composite as potential adsorbent for removal of Abamectin pesticide from wastewater. *Results in Surfaces and Interfaces*, 10(September 2022), 100099. DOI: 10.1016/j.rsurfi.2023.100099.

[28] Mohammed, A.A. (2015). Biosorption of Lead, Cadmium, and Zinc onto Sunflower Shell: Equilibrium, Kinetic, and Thermodynamic Studies. *Iraqi Journal of Chemical and Petroleum Engineering*, 16(1), 91–105. DOI: 10.31699/ijcpe.2015.1.9.

[29] Ghanbari, N., Ghafuri, H. (2023). Preparation of novel Zn–Al layered double hydroxide composite as adsorbent for removal of organophosphorus insecticides from water. *Scientific Reports*, 13(1), 1–15. DOI: 10.1038/s41598-023-37070-8.

[30] Hasani, N., Selimi, T., Mele, A., Thaçi, V., Halili, J., Berisha, A., Sadiku, M. (2022). Theoretical, Equilibrium, Kinetics and Thermodynamic Investigations of Methylene Blue Adsorption onto Lignite Coal. *Molecules*, 27(6) DOI: 10.3390/molecules27061856.

[31] Ali Hammood, Z., Mohammed, A.A. (2024). Adsorption of tetracycline from an aqueous solution on a CaMgAl-layer double hydroxide/red mud composite: Kinetic, isotherm, and thermodynamic studies. *Environmental Nanotechnology, Monitoring & Management*, 22(October), 101018. DOI: 10.1016/j.enmm.2024.101018.

[32] Kuang, H., Zhang, H., Liu, X., Chen, Y., Zhang, W., Chen, H., Ling, Q. (2022). Microwave-assisted synthesis of NiCo-LDH/graphene nanoscrolls composite for supercapacitor. *Carbon*, 190, 57–67. DOI: 10.1016/j.carbon.2021.12.097.

[33] Hassanjani-roshan, A., Emadoddin, E., Vaezi, M., Koohestani, H. (2025). Synthesis of polystyrene colloidal nanoparticles and investigation of their hydrophobic properties on the flotation of phosphorus. *Vietnam Journal of Chemistry*, 63(3), 398–404. DOI: 10.1002/vjch.202400238.

[34] Wibiyan, S., Royani, I., Lesbani, A. (2023). Synthesis and Performance of ZnAl @ Layered Double Hydroxide Composites with Eucheuma cottonii for Adsorption and Regeneration of Congo Red Dye. *Indonesian Journal of Environmental Management and Sustainability*, 8(3), 126–134. DOI: 10.26554/ijems.2024.8.3.126-134.

[35] Mohammed, A.A., Al-Musawi, T.J., Kareem, S.L., Zarrabi, M., Al-Ma'abreh, A.M. (2020). Simultaneous adsorption of tetracycline, amoxicillin, and ciprofloxacin by pistachio shell powder coated with zinc oxide nanoparticles. *Arabian Journal of Chemistry*, 13(3), 4629–4643. DOI: 10.1016/j.arabjc.2019.10.010.

[36] Liu, X. (2021). IR Spectrum and Characteristic Absorption Bands. In: *Organic Chemistry 1*. p. 6.3.1.

[37] Ikemoto, Y., Harada, Y., Tanaka, M., Nishimura, S.N., Murakami, D., Kurahashi, N., Moriwaki, T., Yamazoe, K., Washizu, H., Ishii, Y., Torii, H. (2022). Infrared Spectra and Hydrogen-Bond Configurations of Water Molecules at the Interface of Water-Insoluble Polymers under Humidified Conditions. *Journal of Physical Chemistry B*, 126 (22), 4143–4151. DOI: 10.1021/acs.jpcb.2c01702.

[38] Mohadi, R., Juleanti, N., Normah, N., Mega, P., Bahar, S., Siregar, N., Wijaya, A., Palapa, N.R., Lesbani, A. (2022). 1523 Low-Cost Yet High-Performance Hydrochar Derived from Hydrothermal Carbonization of Duku Peel (Lansium domesticum) for Cr (VI) Removal from Aqueous Solution. *Indonesian Journal of Chemistry*, 22(6), 1523–1533. DOI: 10.22146/ijc.73353.

[39] Altalhi, A.A., Mohamed, E.A., Negm, N.A. (2024). Recent advances in layered double hydroxide (LDH)-based materials: fabrication, modification strategies, characterization, promising environmental catalytic applications, and prospective aspects. *Energy Advances*, 2136–2151. DOI: 10.1039/d4ya00272e.

[40] Huang, Y., Yin, W., Zhao, T.L., Liu, M., Yao, Q.Z., Zhou, G.T. (2023). Efficient Removal of Congo Red, Methylene Blue and Pb(II) by Hydrochar–MgAlLDH Nanocomposite: Synthesis, Performance and Mechanism. *Nanomaterials*, 13(7) DOI: 10.3390/nano13071145.

[41] Alnasrawi, F.A., Mohammed, A.A., Tariq, A.M. (2023). Synthesis and application of layered double hydroxides as a superior adsorbent for the removal of hazardous contaminants from aqueous solutions: a comprehensive review. *Desalination and Water Treatment*, 297, 26–74. DOI: 10.5004/dwt.2023.29579.

[42] Nava-Andrade, K., Carbajal-Arízaga, G.G., Obregón, S., Rodríguez-González, V. (2021). Layered double hydroxides and related hybrid materials for removal of pharmaceutical pollutants from water. *Journal of Environmental Management*, 288(January) DOI: 10.1016/j.jenvman.2021.112399.

[43] Dawood, D.S., Alwared, A.I., Alkhazraji, S.S., Abdul-Majeed, W.S. (2024). Optimization of Pb (II) Ion Removal from Synthetic Wastewater Using Dead (Chlorophyta) Macroalgae: Prediction by RSM Method. *Iraqi Journal of Chemical and Petroleum Engineering*, 25(1), 129–140. DOI: 10.31699/ijcpe.2024.1.13.

[44] Shafiq, M., Alazba, A.A., Amin, M.T. (2023). Preparation of ZnMgAl-Layered Double Hydroxide and Rice Husk Biochar Composites for Cu(II) and Pb(II) Ions Removal from Synthetic Wastewater. *Water (Switzerland)*, 15(12) DOI: 10.3390/w15122207.

[45] Li, M., Wu, G., Liu, Z., Xi, X., Xia, Y., Ning, J., Yang, D., Dong, A. (2020). Uniformly coating ZnAl layered double oxide nanosheets with ultra-thin carbon by ligand and phase transformation for enhanced adsorption of anionic pollutants. *Journal of Hazardous Materials*, 397(April), 122766. DOI: 10.1016/j.jhazmat.2020.122766.

[46] Musah, M., Azeh, Y., Mathew, J., Umar, M., Abdulhamid, Z., Muhammad, A. (2022). Adsorption Kinetics and Isotherm Models: A Review. *Caliphate Journal of Science and Technology*, 4(1), 20–26. DOI: 10.4314/cajost.v4i1.3.

[47] Wang, J., Guo, X. (2022). Rethinking of the intraparticle diffusion adsorption kinetics model: Interpretation, solving methods and applications. *Chemosphere*. 309, Part 2, 136732. DOI: 10.1016/j.chemosphere.2022.136732.

[48] Sulaymon, A.H., Mohammed, A.A., Al-Musawi, T.J. (2014). Multicomponent Biosorption of Heavy Metals Using Fluidized Bed of Algal Biomass. *Journal of Engineering*, 19(4), 469–484. DOI: 10.31026/j.eng.2013.04.05.

[49] Lei, T., Li, S.-J., Jiang, F., Ren, Z.-X., Wang, L.-L., Yang, X.-J., Tang, L.-H., Wang, S.-X. (2019). Adsorption of Cadmium Ions from an Aqueous Solution on a Highly Stable Dopamine-Modified Magnetic Nano-Adsorbent. *Nanoscale Research Letters*, 14(1), 352. DOI: 10.1186/s11671-019-3154-0.

[50] Cholico-González, D., Ortiz Lara, N., Fernández Macedo, A.M., Chavez Salas, J. (2020). Adsorption Behavior of Pb(II), Cd(II), and Zn(II) onto Agave Bagasse, Characterization, and Mechanism. *ACS Omega*, 5(7), 3302–3314. DOI: 10.1021/acsomega.9b03385.

[51] Rejeki, A.T., Istiningrum, R.B. (2020). Adsorption of Cd(II), Pb(II) and Cu(II) from multi-metal aquoeus system by alkali-treated alang-alang grass (Imperata cylindrica). p. 030033. *AIP Conference Proceedings*. 2229 (1), 030033. DOI: 10.1063/5.0002609.

[52] Pelalak, R., Heidari, Z., Khatami, S.M., Kurniawan, T.A., Marjani, A., Shirazian, S. (2021). Oak wood ash/GO/Fe3O4 adsorption efficiencies for cadmium and lead removal from aqueous solution: Kinetics, equilibrium and thermodynamic evaluation. *Arabian Journal of Chemistry*, 14(3), 102991. DOI: 10.1016/j.arabjc.2021.102991.

[53] Tho, P.T., Van, H.T., Nguyen, L.H., Hoang, T.K., Ha Tran, T.N., Nguyen, T.T., Hanh Nguyen, T.B., Nguyen, V.Q., Le Sy, H., Thai, V.N., Tran, Q.B., Sadeghzadeh, S.M., Asadpour, R., Thang, P.Q. (2021). Enhanced simultaneous adsorption of As(iii), Cd(ii), Pb(ii) and Cr(vi) ions from aqueous solution using cassava root husk-derived biochar loaded with ZnO nanoparticles. *RSC Advances*, 11(31), 18881–18897. DOI: 10.1039/d1ra01599k.

[54] Herath, A., Layne, C.A., Perez, F., Hassan, E.B., Pittman, C.U., Mlsna, T.E. (2021). KOH-activated high surface area Douglas Fir biochar for adsorbing aqueous Cr(VI), Pb(II) and Cd(II). *Chemosphere*, 269, 128409. DOI: 10.1016/j.chemosphere.2020.128409.

[55] Fu, C., Zhu, X., Dong, X., Zhao, P., Wang, Z. (2021). Study of adsorption property and mechanism of lead(II) and cadmium(II) onto sulfhydryl modified attapulgite. *Arabian Journal of Chemistry*, 14(2), 102960. DOI: 10.1016/j.arabjc.2020.102960.

[56] Ramutshatsha-Makhwedzha, D., Mbaya, R., Mavhungu, M.L. (2022). Application of Activated Carbon Banana Peel Coated with Al2O3-Chitosan for the Adsorptive Removal of Lead and Cadmium from Wastewater. *Materials*, 15(3), 860. DOI: 10.3390/ma15030860.

[57] Hossain, M.T., Khandaker, S., Bashar, M.M., Islam, A., Ahmed, M., Akter, R., Alsukaibi, A.K.D., Hasan, M.M., Alshammari, H.M., Kuba, T., Awual, M.R. (2022). Simultaneous toxic Cd(II) and Pb(II) encapsulation from contaminated water using Mg/Al-LDH composite materials. *Journal of Molecular Liquids*, 368, 120810. DOI: 10.1016/j.molliq.2022.120810.

[58] Pang, Y., Zhao, C., Li, Y., Li, Q., Bayongzhong, X., Peng, D., Huang, T. (2022). Cadmium adsorption performance and mechanism from aqueous solution using red mud modified with amorphous MnO2. *Scientific Reports*, 12(1), 4424. DOI: 10.1038/s41598-022-08451-2.

[59] Melhi, S. (2023). Recyclable magnetic nanocomposites for efficient removal of cadmium ions from water: performance, mechanism and isotherm studies. *Environmental Pollutants and Bioavailability*, 35(1) DOI: 10.1080/26395940.2022.2163922.

[60] Sami Abboud, A., Ghaffarinejad, A., Mollahosseini, A. (2023). Removal of lead and cadmium ions from wastewater using magnetic alginate impregnated sulfur. *Environmental Nanotechnology, Monitoring and Management*, 20(June), 1–12. DOI: 10.1016/j.enmm.2023.100874.

[61] Li, X., Cui, Y., Du, W., Cui, W., Huo, L., Liu, H. (2024). Adsorption Kinetics and Mechanism of Pb(II) and Cd(II) Adsorption in Water through Oxidized Multiwalled Carbon Nanotubes. *Applied Sciences (Switzerland)*, 14(5) DOI: 10.3390/app14051745.

[62] Osman, H., Uğurlu, M., Vaizoğullar, A.İ., Atasoy, M., Chaudhary, A.J. (2024). Statistical modeling and optimization of heavy metals (Pb and Cd) adsorption from aqueous solution by synthesis of Fe3O4/SiO2/PAM: isotherm, kinetics, and thermodynamic.

[63] Long, X., Zhang, R., Rong, R., Wu, P., Chen, S., Ao, J., An, L., Fu, Y., Xie, H. (2023). Adsorption Characteristics of Heavy Metals Pb2+ and Zn2+ by Magnetic Biochar Obtained from Modified AMD Sludge. *Toxics*, 11(7) DOI: 10.3390/toxics11070590.

[64] Raheem, S.A., Mohammed, A.A. (2025). Efficient removal of Cd(II) and Pb(II) on NiFeAl-LDH@Polystyrene nanocomposite in single and binary systems: Optimization, kinetic and isotherm studies. *Case Studies in Chemical and Environmental Engineering*, 12(September), 101285. DOI: 10.1016/j.cscee.2025.101285.

[65] Sheikh, M.C., Hasan, M.M., Hasan, M.N., Salman, M.S., Kubra, K.T., Awual, M.E., Waliullah, R.M., Rasee, A.I., Rehan, A.I., Hossain, M.S., Marwani, H.M., Islam, A., Khaleque, M.A., Awual, M.R. (2023). Toxic cadmium(II) monitoring and removal from aqueous solution using ligand-based facial composite adsorbent. *Journal of Molecular Liquids*, 389, 122854. DOI: 10.1016/j.molliq.2023.122854.